The Royal Society

Modelling global terrestrial vegetation–climate interaction

Martin Claussen[1*,2], **Victor Brovkin**[1], **Andrey Ganopolski**[1], **Claudia Kubatzki**[1] **and Vladimir Petoukhov**[1]

[1]*Potsdam-Institut für Klimafolgenforschung, Postfach 601203, D-14412 Potsdam, Germany*
[2]*Freie Universität Berlin, Institut für Meteorologie, Germany*

By coupling an atmospheric general circulation model asynchronously with an equilibrium vegetation model, manifold equilibrium solutions of the atmosphere–biosphere system have been explored. It is found that under present-day conditions of the Earth's orbital parameters and sea-surface temperatures, two stable equilibria of vegetation patterns are possible: one corresponding to present-day sparse vegetation in the Sahel, the second solution yielding savannah which extends far into the south-western part of the Sahara. A similar picture is obtained for conditions during the last glacial maximum (21 000 years before present (BP)). For the mid-Holocene (6000 years BP), however, the model finds only one solution: the green Sahara. We suggest that this intransitive behaviour of the atmosphere–biosphere is related to a westward shift of the Hadley–Walker circulation. A conceptual model of atmosphere–vegetation dynamics is used to interpret the bifurcation as well as its change in terms of stability theory.

Keywords: atmosphere–biome interaction, biogeophysical feedback, biome modelling, global atmosphere–biome system

1. INTRODUCTION

In order to explore the impacts of naturally or anthropogenically induced climate variations on human society, it is necessary to understand the Earth's system. This particularly concerns the fragile balance and interaction between the geosphere, the 'abiotic' world, and the biosphere, the living world, which can be defined as together forming the ecosphere. We assume that the fundamental system properties of the ecosphere, such as response mechanisms, regulation ability and adaptability, do not depend on the capacity of the separate subsystems. The subsystems are strongly linked with each other in such a way that the entire system, the ecosphere, behaves as a dynamic totality consisting of coupled, strongly interacting processes of high complexity. While considerable progress has been made in studying the interaction between the atmosphere and the ocean, first steps towards integration of vegetation as an interactive component in a climate model have been undertaken only recently by Henderson-Sellers (1993) and Claussen (1994).

The first attempts to model vegetation–atmosphere interaction at a global scale were made by coupling equilibrium models of vegetation with an atmospheric general circulation model (GCM). For example, Henderson-Sellers (1993) used a modified Holdridge (1947) scheme, and Claussen (1994) used the BIOME model of Prentice *et al.* (1992). These coupled models included only biogeophysical feedbacks, i.e. vegetation changes were related to changes in albedo, roughness length, leaf area index (LAI), etc. Any biogeochemical feedbacks, i.e. the interaction of vegetation changes with changes in the carbon cycle, were not incorporated. This problem has been tackled recently by Betts *et al.* (1997) and Woodward (this volume), for example.

Subsequent studies have applied the coupled atmosphere–equilibrium vegetation models to issues of climate change. For example, deNoblet *et al.* (1996) linked the BIOME model to the LMD (Laboratoire de Météorologie Dynamique, Paris) GCM to examine how changes in the boreal forests and tundra boundary may have contributed to the initiation of glaciation following the Eemian interglacial some 115 000 years ago. Claussen & Gayler (1997) and Kubatzki & Claussen (1997) investigated the influence of the biogeophysical feedback on the climate of the mid-Holocene some 6000 years ago and of the last glacial maximum (LGM), 21 000 years ago, respectively. These model studies have one major limitation. They do not allow for transient vegetation dynamics. Nevertheless, they provide some insight into long-term aspects of vegetation–climate feedbacks. So far they have underscored the importance of incorporating representations of changing vegetation cover within climate models. Last, but not least, they are able to reproduce their own land surface characteristics; hence, they do not have to refer to often sparse palaeogeological and palaeobotanical data for palaeoclimate simulations.

Here we summarize model simulations carried out with the coupled BIOME–ECHAM model. (ECHAM is the atmospheric GCM developed at the Max-Planck Institut für Meteorologie, Hamburg.). We synthesize these simulations by interpreting the changes of model behaviour in

*Author for correspondence (claussen@pik-potsdam.de).

time using a conceptual model of atmosphere–vegetation dynamics.

2. THE ATMOSPHERE–BIOME MODEL

(a) *The atmospheric component*

For the atmospheric component of the combined atmosphere–biome model, we took the climate model ECHAM (v. 3.2) (see Roeckner *et al.* 1992). ECHAM is run at T21 and T42 resolution, hence the Gaussian grid has a resolution of some $5.6^\circ \times 5.6^\circ$ longitude/latitude and some $2.8^\circ \times 2.8^\circ$ longitude/latitude, respectively.

Computation of near-surface transfer of energy, moisture and momentum is based upon the Monin–Obukhov theory as formulated by Louis (1979). Soil moisture is predicted using the bucket-type Arno scheme of Dümenil & Todini (1992), and evaporation using the Blondin (1989) scheme. The latter scheme takes into account vegetation effects such as interception of rain and snow in the canopy, and the stomatal control of evaporation, in a grossly simplified manner. The albedo of snow-covered surfaces depends on the type of vegetation. While the albedo of snow-covered bare soil and grassland can reach 0.4–0.8, depending on temperature, it is restricted to 0.3–0.4 in the case of snow-covered forests. The surface parameters, i.e. the parameters that are defined to control energy and momentum fluxes at the atmosphere–surface interface, such as background albedo, roughness length, vegetation ratio and forest ratio (the relative area of a grid cell covered by vegetation and forest, respectively), and LAI (the area of leaves covering a 1 m^2 surface area), are taken as constant with respect to time, depending only on the biome type (see § 2(*c*) below).

ECHAM is able to simulate the present-day observed time–mean circulation and its intraseasonal variability. Particularly the simulated global distributions of near-surface temperature and precipitation agree well with observations. Differences between seasonal average simulated and observed temperatures are generally smaller than ± 1°C. Exceptions are a cold bias of some -2 °C in the north-west of North America, central Sahara and Siberia during the summer months (June–August), and a cold bias of -4 °C in Siberia during winter (December–February). Concerning precipitation, the structure of the tropical belt is well captured, as are the storm track regions of the Northern Hemisphere. Deviations from observed patterns are found for South Africa and Australia, which receive too much rain during the southern summer (December–February). Moreover, dry regions with a precipitation rate of less then 0.5 mm d^{-1} are more extended than the analysis of Legates & Willmott (1990) suggests. For an extensive report, see Roeckner *et al.* (1992).

(b) *The biome component*

Biomes are computed using the BIOME model (v. 1.0) developed by Prentice *et al.* (1992). This model is based on physiological considerations rather than on mere correlations between climate and biomes as they exist today. Therefore the BIOME model is suitable as a tool to assess changes in natural vegetation in response to changes in climate. However, it is important to note that the BIOME model does not simulate the transient behaviour of vegetation. At best, it predicts constraints within which plant community dynamics could operate.

In the BIOME model, 14 plant functional types are assigned climate tolerances in terms of amplitude and seasonality of climate variables, such as coldest monthly mean temperature, yearly temperature sums, and ratio of actual to equilibrium evapotranspiration. Competition between different plant types is treated indirectly by the application of a dominance hierarchy, which effectively excludes certain types of plants from a site according to the presence of other plants, rather than on account of the climate. Finally, 17 biomes are defined as combinations of dominant types.

Biome patterns computed from a 30-year ECHAM climatology study (Claussen 1997*b*; not shown here) agree fairly well with those derived from Leemans & Cramer's (1991) climate data—corroborating the ability of ECHAM to recapture the global distribution of precipitation and near-surface temperature. The global κ value is close to 0.5. (The kappa statistics are presented by Monserud & Leemans (1992) as an objective tool for comparing global vegetation maps. κ values range from 0 to 1; the smaller the number, the worse the agreement.) Differences between biome maps reflect the above-mentioned regional deficiencies of ECHAM. Too much forest is diagnosed from the ECHAM simulation for Australia. In boreal latitudes, there appears to be a lack of taiga and tundra due to the cold bias of the ECHAM simulation.

(c) *Coupling of the atmospheric and biome components*

ECHAM is asynchronously coupled with the BIOME model: from climate variables computed by ECHAM, biomes are diagnosed with the BIOME model. Subsequently, surface parameters are allocated to biomes. With the new surface parameters, the simulation with ECHAM is continued for some model years—based on earlier investigations (Claussen 1994), six years are chosen from which the first year is omitted as an adjustment period for soil–water transports. From the new simulation biomes are diagnosed again and so on. The sequence of allocation of surface parameters to biomes, integration with ECHAM, and computation of biomes using the BIOME model is referred to as 'iteration'. Several iterations are performed until the biome patterns and the state of the atmosphere no longer reveal any significant trend.

Allocation of surface parameters to biomes is described in Claussen (1994, 1997*a*). The biome 'sand desert', which is not included in the original BIOME model, was introduced to take into account the large differences between albedo values of various types of desert. In the Sahara and Arabian deserts, large patches of high albedo—in some places up to 0.42—are observed by satellite (e.g. Ramanathan *et al.* 1989). Therefore, whenever the BIOME model predicts a desert biome in these regions, 'sand desert' was chosen. In Claussen (1997*b*), 'sand desert' is computed from soil moisture availability (i.e. the ratio of actual to equilibrium evapotranspiration) and surface topography, rather than prescribed by using a 'sand desert mask' specified from satellite data. Use of this (ad hoc) scheme instead of the 'sand desert mask' does not change the main results that are presented in the following sections.

3. RESULTS

(a) *Present-day climate*

The first attempt to couple ECHAM with BIOME brought forth the result that incorporation of the BIOME model does not change the internal variability of the simulated climate significantly (Claussen 1994). Perhaps more importantly, it was found that the atmosphere–vegetation system, or more precisely the atmosphere–biome system, could be an intransitive system, as the coupled ECHAM–BIOME model yields different solutions depending on the initial conditions. A more detailed analysis was given by Claussen (1997*a*) who assessed the problem of the dynamics of deserts and drought in the African and Indian monsoon region, i.e. Sahel, Saudi Arabia, and the Indian subcontinent. It was found that, under present-day conditions of solar irradiation and sea-surface temperatures (SST), two solutions of the atmosphere–biome system are possible: the first solution yields the present-day distribution of vegetation and deserts (figure 1*a*) and the second one shows a northward spread of savannah and xerophytic shrubs of some 600 km, particularly in the south-western Sahara (figure 1*b*). (In figure 1*a*,*b*, we do not present the distribution of all 17 biomes, but we have grouped biomes into four biome groups according to table 1.) Whether the atmosphere–biome model attained the first or the second solution depended on the initial conditions. If a bright sand desert (i.e. a desert with a high albedo of some 35%) is prescribed in the area currently occupied by the Sahara desert, then the atmosphere–biome model keeps the desert. If, however, vegetation is initially specified, then some vegetation (savannah, xerophytic shrub, and steppe) remains in the south-western Sahara.

Claussen's study (Claussen 1997*a*) focused on biogeophysical feedbacks in the tropical and subtropical regions. Vegetation patterns are changed only in these regions. This rather regional study was extended to a global scale (Claussen 1997*b*). It was demonstrated that the ECHAM–BIOME model generally yields two solutions. If the continents are initially covered with sand desert, then the present-day distribution of subtropical deserts appears. However, if the continents are initially covered with dark soil or any type of vegetation (either forest or grassland), then the Sahara and Arabian deserts become smaller; moreover, the climate in central East Asia is less arid. Therefore one can conclude that North Africa is the region which is most sensitive to changes in vegetation cover concerning bifurcations of the atmosphere–biome system in today's climate.

(b) *The last glacial maximum (21 000 years BP)*

Kubatzki (1996) and Kubatzki & Claussen (1997) analysed the biogeophysical feedbacks during the LGM some 21 000 years ago using the ECHAM–BIOME model. During the LGM, the atmospheric CO_2 concentration was lower than it is today, and the sea-surface was generally colder with the exception of some regions in the subtropical Pacific where SSTs were slightly higher than they are today according to the CLIMAP (CLIMAP project members 1981) reconstruction. Moreover, the land–sea distribution was changed owing to the extensive glaciation. The regional distribution of solar radiation, however, was quite similar to today's values. Kubatzki (1996) found that the ECHAM–BIOME model improved the results of ECHAM, the atmosphere-only model in which the present-day land surface was prescribed. Especially in the Siberian region, the inclusion of the vegetation–snow–albedo interaction led to a better agreement with geological reconstructions.

Furthermore, Kubatzki (1996) detected two stable equilibrium solutions of the ECHAM–BIOME model under LGM conditions. As for present-day conditions, the presence of a sand desert at the beginning of a simulation leads to extended subtropical deserts, by and large in agreement with palaeogeological reconstructions (figure 2*a*). However, an inital global vegetation cover of either forest or steppe, or of dark desert with albedo values lower than 0.2, results in a northward spread of vegetation of up to some 1000 km, mainly into the western Sahara (figure 2*b*).

(c) *Mid-Holocene (6000 years BP)*

For the mid-Holocene, the ECHAM–BIOME model simulates a northward shift of savannah up to 20° N into the Sahara, which in turn amplifies the response of the atmospheric circulation to changes in the Earth's orbit during the Holocene (Claussen & Gayler 1997). Moreover, most of the western part of the Sahara appears to be vegetated by xerophytic woods/shrubs and warm grass, while the eastern part remains a desert in the simulation (figure 3*b*). The simulated vegetation distribution agrees better with palaeobotanical reconstructions than results from the same atmospheric model, but only when omitting biogeophysical interaction, i.e. keeping the ECHAM and the BIOME model off-line. If the land surface conditions are kept at present-day values—as required for the Palaeoclimate Modelling Intercomparison Project (PMIP; Joussaume & Taylor 1995)—then the ECHAM model produces a near-surface climate which resembles the present-day climate. At least the biome pattern diagnosed from this simulation (figure 3*a*) is close to today's pattern.

As a surprising result of the mid-Holocene simulation, the ECHAM–BIOME model yields only one equilibrium solution—the 'green' Sahara. In contrast to the present-day and the LGM simulations, the arid Sahara does not appear to be an equilibrium solution. In other words, when initializing the ECHAM–BIOME model with the results from the PMIP simulation for 6000 BP, the model drifts towards the 'green' Sahara solution.

4. SYNTHESIS

The difference between the two solutions of the ECHAM–BIOME model for present-day and LGM climates, as well as between the PMIP simulation and the equilibrium solution for mid-Holocene conditions, can be interpreted in terms of Charney's theory of desertification. Charney (Charney 1975; Charney *et al.* 1975) suggested that a desert is stable because sandy, non-vegetated soil has a much higher albedo than soil covered by vegetation. Therefore, a desert reflects more solar radiation to space than any vegetated area under the same meteorological conditions. Moreover, desert surfaces are hotter than vegetated surfaces, and the air above them is less cloudy.

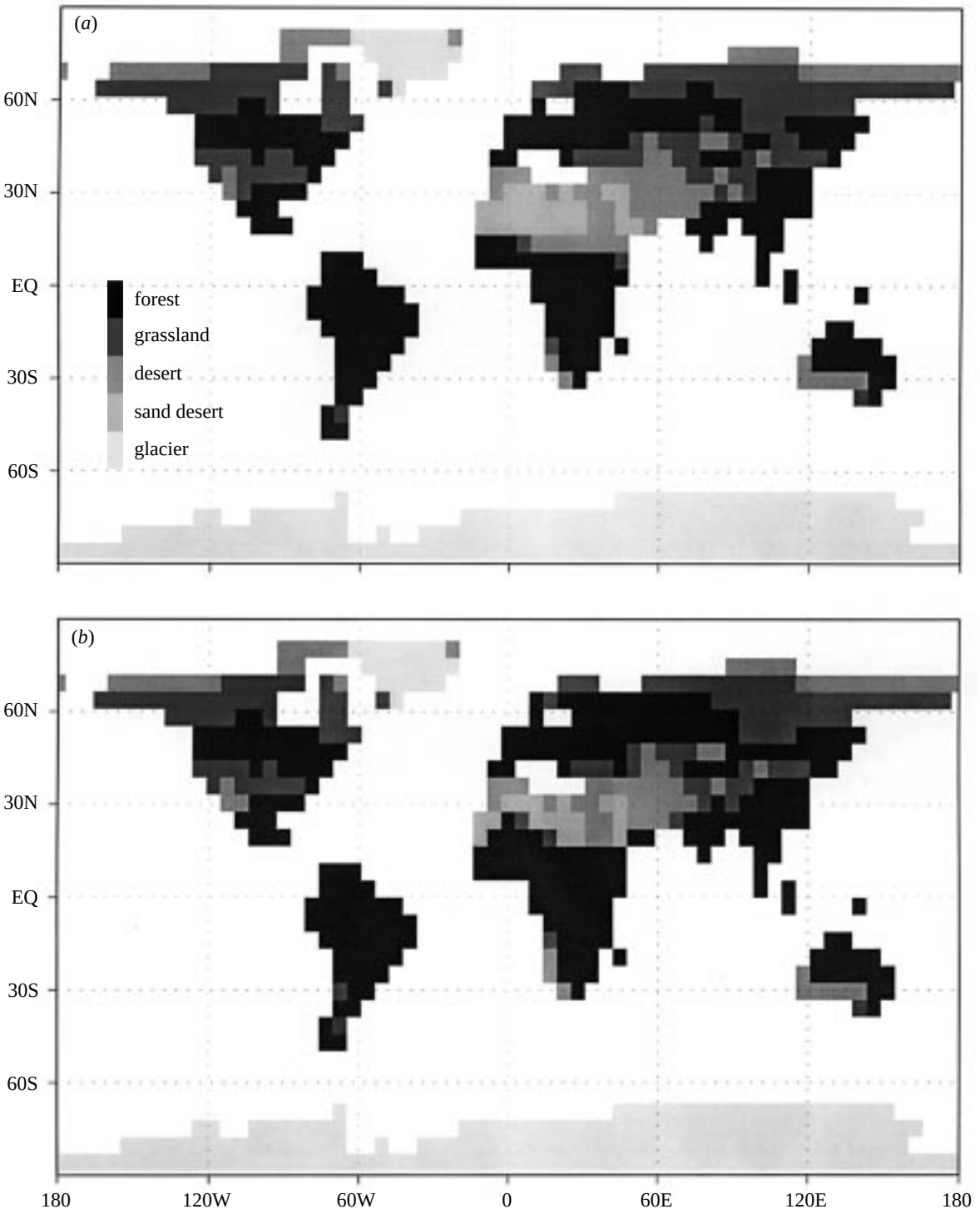

Figure 1. Biome patterns computed from the last iteration of the ECHAM–BIOME model when (*a*) initialized with present-day biome distrubution and (*b*) with an anomalous biome distribution in which tropical forests are replaced by desert and subtropical deserts are replaced by rainforest. The 17 biomes computed by the BIOME model are collected into biome groups (forests, grassland, and desert) according to table 1.

Hence, a desert emits more longwave radiation to space. The net result is that a desert is a radiative sink of heat relative to its surroundings. Because the troposphere above the Sahara is cooler than above the adjacent regions, there is a relative air flow towards the Sahara. The air over the Sahara must descend and compress adiabatically, thereby it becomes warmer and drier. Consequently, the likelihood of precipitation becomes vanishingly small. Moreover, the divergence of near-surface winds becomes stronger over a desert than over a vegetated region. For the Sahel region this implies that the African summer monsoon appears to be weaker in the case of a more widespread desert than in the case of a vegetated Sahel. Or, in other words, in the case of a 'green' Sahara the summer monsoon reaches farther inland. Therefore, convection, i.e. upward motion, shifts northward and

Table 1. *Allocation of biomes defined by Prentice* et al. *(1992) to biome groups used in figures 1–3*

biome	biome group
tropical rain forest	forest
tropical seasonal forest	
savanna	
warm mixed forest	
temperate deciduous forest	
cool mixed forest	
cool conifer forest	
taiga	
cold mixed forest	
cold deciduous forest	
xerophytic woods /shrub	
warm grass / shrub	grassland
cool grass / shrub	
tundra	
hot desert	desert
cool desert	
polar desert	
(no vegetation)	sand desert
	glacier

becomes stronger than in the case of an arid Sahel. (For a more detailed discussion of this mechanism, see Claussen (1997*a*).)

Processes in North Africa and over the Indian subcontinent are coupled with the tropical easterly jet (e.g. Subbaramayya & Ramanadnam 1981), which is found near the tropical tropopause during the boreal summer. The tropical easterly jet reaches from the West Pacific to Africa. It has a main branch crossing the equator and a secondary branch north of the equator. This northern branch is modified by convection. It gets stronger when convection shifts northward as is the case for the 'green' Sahara.

These differences in atmospheric circulation, which are associated with the differences in biome patterns, are conveniently characterized by the so-called velocity potential. The velocity potential has the following meaning. The wind field can be divided into a non-divergent and an irrotational component. Gradients of the velocity potential are proportional to the irrotational, divergent wind. Therefore, the velocity potential is a measure of divergence and convergence of the large-scale atmospheric circulation. Figures 4*a* shows the velocity potential near the tropopause at 200 hPa (i.e. approximately at heights of 10 km) simulated for the present-day climate and normal biome patterns as presented in figure 1*a*. Negative values of the velocity potential over the Philippines and the Chinese Sea indicate a strong divergence of the circulation there. This is caused by convection, i.e. rising air within the troposphere, the lowest 10 km above the warm waters of the West Pacific. The centre of convergence near the tropopause, i.e. the region in which the air descends at a large-scale, is located over South Africa in the present-day climate. This dipole pattern of velocity potential reflects the tropical Hadley–Walker circulation.

In the (anomalous) case of a smaller Sahara desert (figure 1*b*) the centre of convergence shifts westward to the tropical Atlantic (figure 4*b*). The same qualitative shift of veloctiy potential can be shown for the LGM simulations (not presented here). Also for mid-Holocene conditions, the difference between the PMIP simulation and the simulation with the coupled ECHAM–BIOME model yields a similar dipole structure (figure 5*a*).

If the differences in atmospheric circulation between the 'dry' solutions and the 'green' solutions look similar for all simulations, how can one explain that the vegetation pattern resulting from the PMIP simulation is not a stable solution of the ECHAM–BIOME model? Boundary conditions such as atmospheric CO_2 concentration, land–sea distribution, SST, and inland ice distribution differ between the present-day and LGM simulations, but were kept at the same values for the present-day and mid-Holocene simulations. However, the radiative forcing owing to changes in Earth's orbital parameters differs strongly between the present-day and LGM climate on the one hand and the mid-Holocene climate on the other hand. During the mid-Holocene, the tilt of the Earth's axis was 0.7° stronger than it is today, and the perihelion was in mid-September. As a result, the solar radiation during the boreal summer increased by some 30 W m^{-2} at 60° N (e.g. Kutzbach & Guetter 1986) thereby increasing the large-scale temperature contrast between the Eurasian continent and the oceans and, according to Kutzbach & Guetter (1986), amplifying the African and Indian summer monsoons.

Changes in the large-scale atmospheric circulation between present-day and mid-Holocene conditions owing to orbital forcing only, and expressed in terms of velocity potential, are depicted in figure 5*b*. It appears that orbital forcing alone increases the divergence above South-East Asia and shifts the convergence westward. (In figure 5*b*, a strong increase in convergence is seen over the South-East Pacific, but there is also a secondary maximum over the tropical Atlantic.) Quite a similar shift was found by deNoblet *et al*. (1996) when comparing present-day and mid-Holocene velocity potentials owing to orbital forcing. Hence, orbital forcing already causes a westward shift of the Hadley–Walker circulation, and the biogeophysical feedback just amplifies it. Therefore, we suggest that orbital forcing prevents the atmospheric circulation from locking into the 'dry' mode, simply because the African and Indian monsoons and associated moisture advection into these regions become too strong to sustain a desert Sahara.

The comprehensive ECHAM–BIOME model provides a wealth of details about feedbacks between equilibrium vegetation structure and the atmospheric circulation. To understand the stability of the atmosphere–biome system more generally, we have reduced the comprehensive model to a conceptual one which is more easily accessible to the mathematical theory of stability. Since this work has not yet been completed, we present only the basic outline of it to stimulate further discussion on this subject.

Assuming that in the Sahel, vegetation mainly depends on precipitation, one may parameterize this dependence by

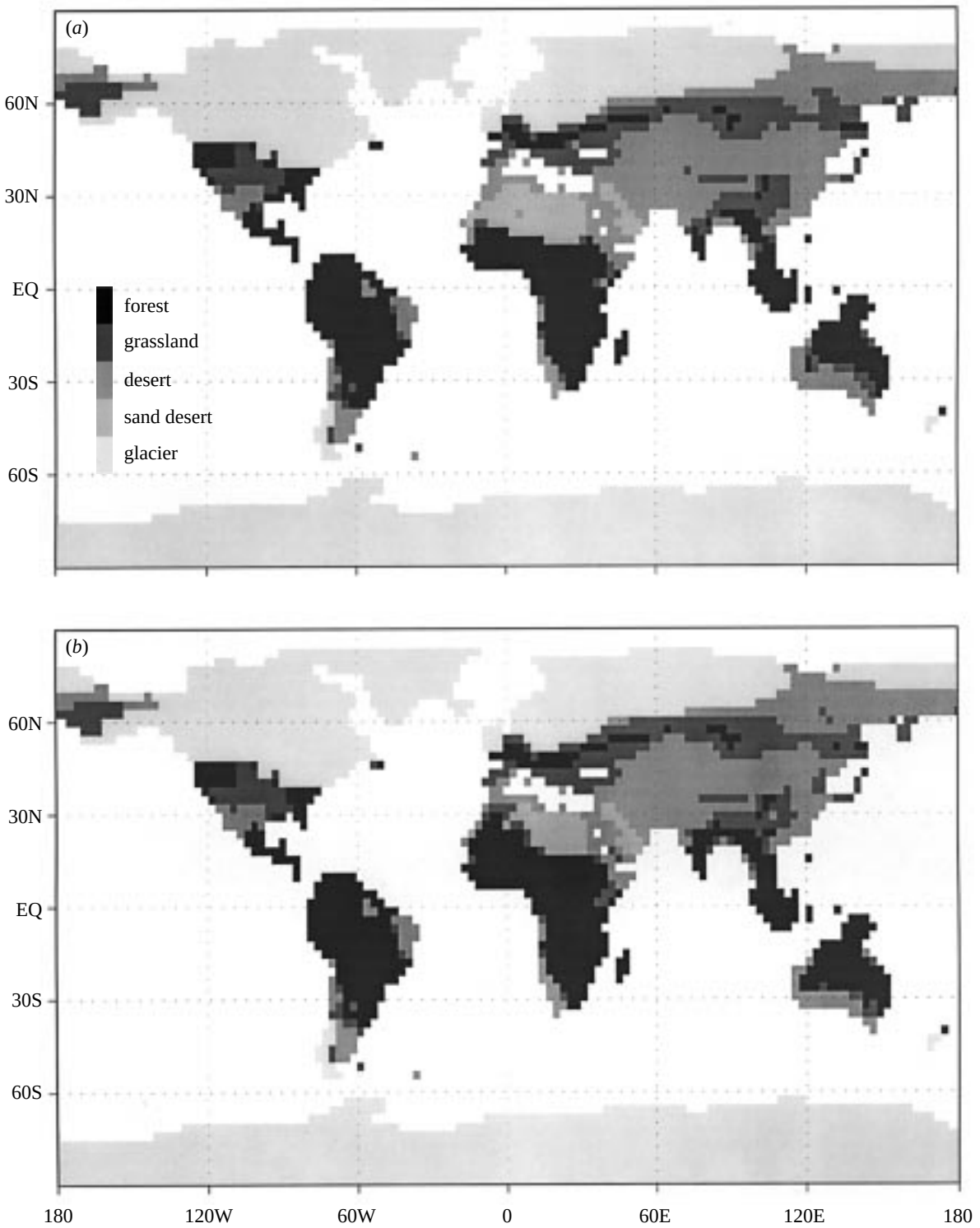

Figure 2. Biome patterns computed by the ECHAM–BIOME model for the last glacial maximum (LGM). All land surfaces are initially covered by (*a*) sand desert and (*b*) rainforest. Results similar to (*a*) are obtained if the ECHAM–BIOME model is initialized with present-day land-surface conditions. The 17 biomes computed by the BIOME model are collected into biome groups (forests, grassland, and desert) according to table 1.

$$V^*(P) = \begin{cases} 0 & \text{if } P \leqslant P_{\mathrm{cr}} \\ 1 - \dfrac{1}{1 + a(P - P_{\mathrm{cr}})^2} & \text{if } P > P_{\mathrm{cr}} \end{cases} \qquad (1)$$

where V^* is the vegetation fraction being in equilibrium with climate, here given in terms of annual mean precipitation P. P_{cr} is a threshold value of annual mean precipitation below which no vegetation can exist in the long-term. A typical value for P_{cr} in the Sahel is roughly $100\,\mathrm{mm\,yr^{-1}}$. The hyperbolic curve (equation (1)) merely states that there is little change in the vegetation fraction if precipitation is small. Once vegetation is close to saturation (V^* being close to unity), then any increase in precipitation will have little effect on the vegetation fraction. Between these states one could choose any reasonable interpolation, be it linear or exponential or hyperbolic.

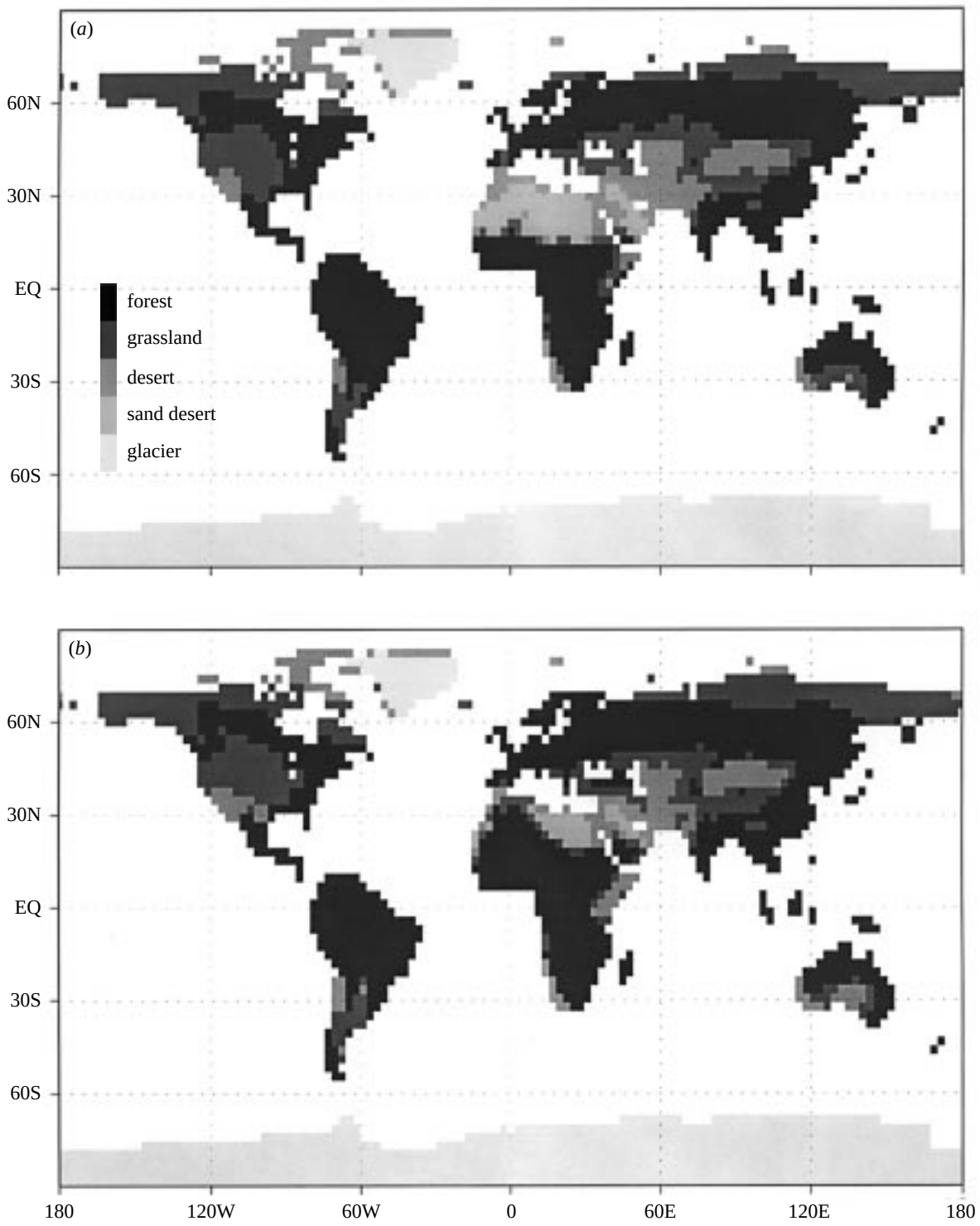

Figure 3. Biome patterns computed for the mid-Holocene. (*a*) Results obtained from the atmosphere-only model ECHAM in which all land surfaces are kept at present-day values. (*b*) Results from the coupled ECHAM–BIOME model. The 17 biomes computed by the BIOME model are collected into biome groups (forests, grassland, and desert) according to table 1.

The reponse of the African monsoon, given in terms of precipitation P, on changes in the vegetation fraction V in the Sahel is written, for simplicity, as a linear model:

$$P(V) = P_{\mathrm{I}} + bV. \qquad (2)$$

Parameters a, b, P_{cr}, P_{I} are obtained by fitting equation (1) to the ecological data of Olson *et al.* (1983) and climate data of Leemans & Cramer (1991), and equation (2) to the ECHAM–BIOME model output.

The conceptual model yields either one or three solutions (V_0, P_0)—the intersection points of equations (1) and (2)—mainly depending on the parameter $P_{\mathrm{I}} - P_{\mathrm{cr}}$. Work in progress suggests that b attains similar values for all simulations, and that $P_{\mathrm{I}} - P_{\mathrm{cr}} < 0$ for the present-day and LGM monsoon, but $P_{\mathrm{I}} - P_{\mathrm{cr}} > 0$ for the mid-

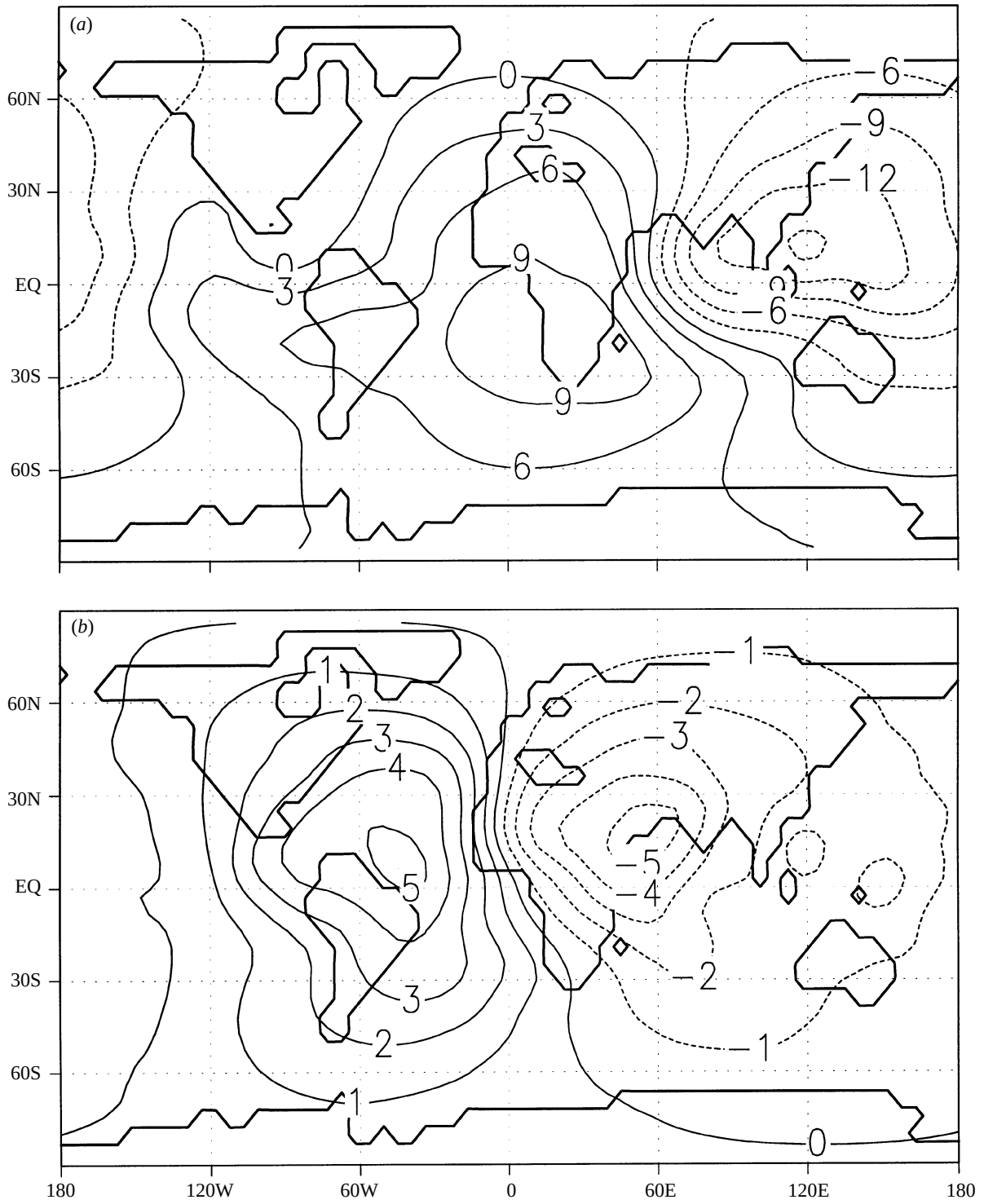

Figure 4. Global distribution of velocity potential near the top of the tropopause at 200 hPa (i.e. at heights of some 10 km) for the present-day climate. (*a*) Results taken from the simulation which is initialized with present-day biome distribution and which yields biome patterns presented in figure 1*a*. (*b*) Differences in velocity potential between the simulation of today's climate and the simulation initialized with the anomalous biome pattern, which leads to the biome distribution shown in figure 1*b*.

Holocene climate. Hence, the conceptual model yields one 'green' solution for the mid-Holocene, but three (one 'desert' solution, one 'green' solution, and one in between 'desert' and 'green') for the present-day and LGM conditions.

At first glance this seems to contradict the results of the ECHAM–BIOME model, which exhibits either one or only two solutions. However, stability analysis reveals that one out of three solutions is always unstable. Assuming that vegetation responds to changes in climate with some relaxation time t_r, one may write that

$$\frac{dV}{dt} = \frac{1}{t_r}(V^*(P) - V) \qquad (3)$$

By combining equations (1)–(3) and linearizing equation (3) with respect to small perturbations in the vegetation fraction around any equilibrium solution, one finds that

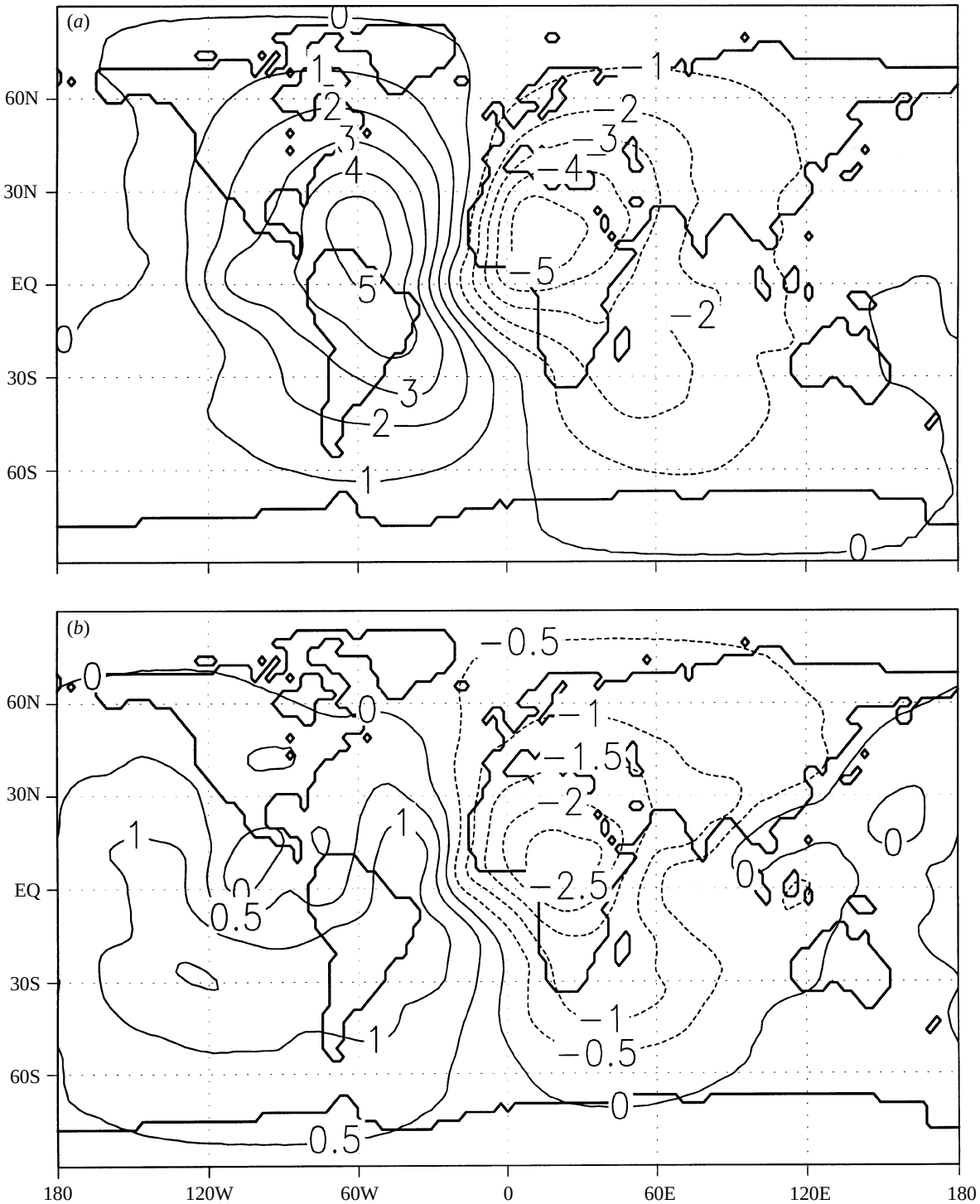

Figure 5. Global distribution of differences in velocity potential near the top of the tropopause at 200 hPa for the mid-Holocene. (*a*) Differences between the atmosphere-only model, ECHAM, and the coupled ECHAM–BIOME model. (*b*) Differences between simulations of present-day and mid-Holocene climate using the atmosphere-only model.

the solution $(V_0^{\mathrm{u}}, P_0^{\mathrm{u}})$ for which the slope of the curve of equation (1) is larger than the slope of equation (2) is unstable. (This is an application of the more general so-called 'slope-stability theorem' (see North *et al.* 1981), which applies to many relaxation problems.)

5. CONCLUSIONS

Coupling the equilibrium vegetation model BIOME by Prentice *et al.* (1992) with the ECHAM model yields multiple equilibrium solutions. Under present-day conditions of the Earth's orbital parameters and SSTs, two stable equilibria of vegetation patterns are possible: one corresponding to present-day sparse vegetation in the Sahel, the second solution yielding savannah extending far into the south-western part of the Sahara. Similar conclusions are obtained for conditions during the last glacial maximum (21 000 years BP). For the mid-Holocene (6000 years BP), however, the model finds only one solution: the 'green' Sahara.

Analysis of atmospheric circulations reveals that the difference between 'dry' and 'green' solutions is associated with a westward shift of the Hadley–Walker circulation. In the case of a more vegetated North Africa, the divergence of the large-scale flow in the upper troposphere over the south-east Asian region becomes stronger. So does the convergence; moreover, the latter shifts northwest towards the tropical Atlantic. In the mid-Holocene, this shift occurs already as a result of an increase in summer solar radiation on the Eurasian continent owing to changes in the Earth's orbit. Associated with it is a stronger African and Indian summer monsoon. The biogeophysical feedback just amplifies this effect. Therefore, we suggest that orbital forcing is responsible for locking the atmosphere–biome system into the 'green' mode.

While the comprehensive ECHAM–BIOME model provides details of the interaction between vegetation and atmospheric circulation, a conceptual model is used to interpret the existence of multiple solutions as well as their stability. In the conceptual model, the dependence of equilibrium vegetation on changes in annual mean precipitation is parameterized; furthermore, the strength of the African monsoon in terms of precipitation is assumed to be a linear function of vegetation cover in the Sahel. The linear model is fitted to output from the comprehensive model. The conceptual model demonstrates that the atmosphere–biome system may reveal only one 'green' solution, if owing to some external forcing the monsoon precipitation over sparsely vegetated areas in the Sahel, P_1 in the conceptual model, exceeds the threshold P_{cr} of annual mean precipitation, below which no vegetation can exist in the Sahel. In the present-day and LGM climate, $P_1 - P_{cr} < 0$, such that the conceptual model obtains three solutions, one of which is, however, unstable to small perturbations in the vegetation fraction.

A conceptual model of atmosphere–vegetation dynamics does not prove the existence of multiple equilibrium solutions of the atmosphere–biome system, but it helps to interpret results obtained from the comprehensive model. More (numerical) experiments using different comprehensive models have to be undertaken to confirm the possibility of multiple equilibrium solutions.

If it turns out that the atmosphere–biome system can attain multiple equilibrium states, one has to ask why nature 'picks' the one and not the other solution—or why does the Sahara appear to be a desert in the present-day climate, although it could be green in at least some parts? Equilibrium vegetation–atmosphere models are not really suited to answering this question. These models do not include biogeochemical feedbacks such as reactions of vegetation composition to changes of atmospheric CO_2 concentration, and, perhaps more importantly, they do not take into account ocean dynamics. It is known that temperatures of the tropical Atlantic are correlated with Sahelian rainfall (e.g. Lamb & Peppler 1992). Hence, it is not completely unrealistic to hypothesize a feedback between African monsoon and oceanic circulation in the tropical Atlantic. Therefore, we cannot fully explore the role of vegetation in the climate system until coupled models of vegetation–atmosphere–ocean circulation have been developed.

The authors thank Colin Prentice, Department of Plant Ecology, Lund University, Sweden, for making the BIOME model available. We also thank the Royal Society and the organizers of this Discussion Meeting. Alison Schlums edited the manuscript. Part of the work was done while M.C. and C.K. were at the Max-Planck Institut für Meteorologie in Hamburg.

REFERENCES

Betts, R. A., Cox, P. M., Lee, S. E. & Woodward, F. I. 1997 Contrasting physiological and structural vegetation feedbacks in climate change simulations. *Nature* **387**, 796–799.

Blondin, C. 1989 Research on land surface parameterization schemes at ECMWF. In *Proceedings of the workshop on 'Parameterziation of fluxes over land surfaces'*. Reading, UK: ECMWF.

Charney, J. G. 1975 Dynamics of deserts and drought in the Sahel. *Q. J. R. Met. Soc.* **101**, 193–202.

Charney, J. G., Stone, P. H. & Quirk, W. J. 1975 Drought in the Sahara: a biogeophysical feedback mechanism. *Science* **187**, 434–435.

Claussen, M. 1994 On coupling global biome models with climate models. *Clim. Res.* **4**, 203–221.

Claussen, M. 1997*a* Modeling biogeophysical feedback in the African and Indian Monsoon region. *Clim. Dynamics* **13**, 247–257.

Claussen, M. 1997*b* On multiple solutions of the atmosphere–vegetation system in present-day climate. *Global Change Biol.* (In the press.)

Claussen, M. & Gayler, V. 1997 The greening of Sahara during the mid-Holocene: results of an interactive atmosphere–biome model. *Global Ecol. Biogeogr. Lett.* (In the press.)

CLIMAP project members 1981 *Seasonal reconstruction of the Earth's surface at the last glacial maximum*. Geological Society of America, Map Chart Series, MC-36. Boulder, CO: Geological Society of America.

deNoblet, N., Prentice, I. C., Jousaume, S., Texier, D., Botta, A. & Haxeltine, A. 1996 Possible role of atmosphere–biosphere interactions in triggering the last glaciation. *GRL* **23**(22), 3191–3194.

Dümenil, L. & Todini, E. 1992 A rainfall run-off scheme for use in the Hamburg GCM. In *Advances in theoretical hydrology* (ed. J. P. O'Kane), pp. 129–157. European Geophysical Society Series on Hydrological Sciences, vol. 1. Amsterdam: Elsevier.

Henderson-Sellers, A. 1993 Continental vegetation as a dynamic component of a global climate model: a preliminary assessment. *Clim. Change* **23**, 337–378.

Holdridge, L. R. 1947 Determination of world plant formations from simple climatic data. *Science* **105**, 367–368.

Joussaume, S. & Taylor, K. 1995 Status of the paleoclimate modeling intercomparison project. In *Proceedings of the first international AMIP scientific conference*, pp. 425–430. WCRP report.

Kubatzki, C. 1996 *Numerische experimente zu den globalen biogeophysikalischen wechselwirkungen während des letzten glazialen maximums (21 000 jahre vor heute)*. Diploma thesis, University of Hamburg, Germany.

Kubatzki, C. & Claussen, M. 1997 Simulation of the global biogeophysical interactions during the last glacial maximum. *Clim. Dynamics*. (Submitted.)

Kutzbach, J. E. & Guetter, P. J. 1986 The influence of changing orbital parameters and surface boundary conditions on climate simulations for the past 18 000 years. *J. Atmos. Sci.* **43**, 1726–1759.

Lamb, P. J. & Peppler, R. A. 1992 Further case studies of tropical Atlantic surface atmospheric and oceanic patterns associated with sub-Saharan drought. *J. Climatol.* **5**, 476–487.

Leemans, R. & Cramer, W. 1991 *The IIASA database for mean monthly values of temperature, precipitation, and cloudiness on a global terrestrial grid.* IIASA Research Report RR-91-18, Laxenburg, Austria.

Legates, D. R. & Willmott, C. J. 1990 Mean seasonal and spatial variability in gauge corrected global precipitation. *J. Climatol.* **10**, 111–127.

Louis, J. F. 1979 A parametric model of vertical eddy fluxes in the atmosphere. *Boundary-Layer Meteorol.* **17**, 187–202.

Monserud, R. A. & Leemans, R. 1992 Comparing global vegetation maps with the Kappa statistic. *Ecol. Model.* **62**, 275–293.

North, G. R., Cahalan, R. F. & Coakley, J. A. Jr 1981 Energy balance climate models. *Rev. Geophys. Space Phys.* **19**, 91–121.

Olson, J. S., Watts, J. A. & Allison, L. J. 1983 *Carbon in live vegetation of major world ecosystems.* ORNL-5862, Oak Ridge National Laboratory.

Prentice, I. C., Cramer, W., Harrison, S. P., Leemans, R., Monserud, R. A. & Solomon, A. M. 1992 A global biome model based on plant physiology and dominance, soil properties and climate. *J. Biogeogr.* **19**, 117–134.

Ramanathan, V., Cess, R. D., Harrison, E. F., Minis, P., Barkstrom, B. R., Ahmad, E. & Hartmann, D. 1989 Cloud-radiative forcing and climate: results from the Earth Radiation Budget Experiment. *Science* **243**, 57–63.

Roeckner, E. (and 13 others) 1992 *Simulation of the present-day climate with the ECHAM model: impact of model physics and resolution.* Report 93. Hamburg, Germany: Max-Planck Institut für Meteorologie.

Subbaramayya, I. & Ramanadnam, R. 1981 On the onset of the Indian southwest monsoon and the monsoon general circulation. In *Monsoon dynamics* (ed. J. Lighthill & R. Pearce), pp. 213–220. Cambridge University Press.

Discussion

F. A. Street-Perrott (*Department of Geography, University of Wales, Swansea, UK*). The existence of two alternative stable climate states in the Sahara–Sahel region would help to explain the very abrupt changes in climate and vegetation seen in the Holocene; for example, the rapid desiccation of the Nigerian Sahel shortly after 4000 calendar years ago, which resulted in a dramatic reduction in the representation of arboreal pollen in lake sediments, or the prolonged (interdecadal) periods of drought observed in the twentieth century, which alternate with prolonged wetter periods.

M. Claussen. The abrupt change from a 'green' Sahara to a desert, as we observe it today, could indeed be caused by a change in the stability of the atmosphere–biome system. If we compute the potential function derived from the conceptual model, we see that for 6000 Ma BP, there is only one globally stable solution, the 'green' Sahara. For present-day conditions, the 'green' Sahara is still stable, but the 'desert' solution is more stable. Any large-scale perturbation in the vegetation fraction, perhaps caused by a prolonged drought, will take the system from a 'green' to a 'dry' Sahara.

Whether the interdecadal periods of dry and wet phases in the Sahel could be contributing to this bifurcation remains to be investigated. I would assume that the climate variability in the Sahel is related to changes in the oceanic circulation, for example, El Niño on short time-scales and the conveyor belt on long time-scales.